

Chuixiang Yi¹, Russell K. Monson¹, Zhiqiang Zhai², Dean E. Anderson³, Andrew A. Turnipseed^{1,4}, Sean P. Burns¹, Brian Lamb⁵

¹Department of Ecology and Evolutionary Biology, University of Colorado, Boulder, CO 80309-0334, USA

²Department of Ecology and Evolutionary Biology, University of Colorado, Boulder, CO 80309-0334, USA

³U.S. Geological Survey, Water Resources Division, Denver Federal Center, Lakewood, CO 80225, USA

⁴Atmospheric Chemistry Division, National Center for Atmospheric Research, Boulder, CO 80305, USA.

⁵Laboratory for Atmospheric Research, Washington State University, Pullman, WA 99164-2910, USA

1. Introduction

The exchange of materials and energy between plant canopies and the atmosphere underlies some of the most important environmental challenges facing humankind, including perturbations to the global carbon cycle, the introduction of pollutants into the atmosphere and the transfer of water from soil and vegetation to the atmosphere. Land-atmosphere exchange is the key link between biosphere and atmosphere. During the past decade tower flux networks have flourished for monitoring land-atmosphere exchange by the eddy covariance approach. The Fluxnet tower network includes 368 sites as of October 2005. The eddy covariance approach is most accurate when applied to ecosystems with flat topography and homogeneous vegetation cover (Baldocchi et al., 2001; Goulden et al., 1996). However, many Fluxnet sites are located in complex terrain where topographic advection errors can be the same order as the eddy flux itself (Finnigan, 2004; Massman and Lee, 2002; Goulden et al., 2006). Networks of flux towers are now vital to provide the empirical constraint required for accurate regional and global carbon budget modeling. However, advection caused by topography and surface heterogeneity remains a serious obstacle to routine 24 hour operation for eddy flux towers. An international workshop (held in Boulder 26-28 January 2006) organized by the eddy flux research community defined advective flows as 'difficult conditions' in flux measurements (Finnigan 2006; Mahrt, 2006; Feigenwinter, 2006).

In this presentation, we reprot significant progress in modeling canopy flows over complex terrain and in understanding how topographical flow influences CO₂ flux measurements (Yi et al., 2005; 2006). This progress has been accomplished using data collected at the Niwot Ridge Ameriflux site which contains: (1) a nested design of four towers (within 150 m of each other), (2) three temporal towers along a prominent topographic drainage, each with vertical profiling of CO₂,

wind speed and wind direction, (3) two towers with continuous flux measurements of CO₂, H₂O, and energy, and (4) SF₆ diffusion experiments and leaf area density measurements.

2. Results

2.1. The analytical models that predicts canopy drainage flows and canopy turbulence (Yi et al., 2005)

The drainage flow model is described by

$$u^{\pm}(z) = \pm \left(e^{-(LAI-L(z))} \frac{c_D^h}{c_D(z)} u_h^2 - g \frac{\Delta\theta \sin \alpha}{\theta_0 c_D(z)} \int_z^h e^{-(L(z')-L(z))} dz' \right)^{\frac{1}{2}} \quad (1)$$

and the momentum flux model by

$$-\overline{u'w'}(z) = -\overline{u'w'}(h) e^{-(LAI-L(z))} - g \frac{\Delta\theta}{\theta_0} \sin \alpha \int_z^h e^{-(L(z')-L(z))} dz' \quad (2)$$

Where $L(z) = \int_0^z \ell(z') dz'$ is a layer leaf area

from ground to height z , $\ell(z)$ is leaf area density, g is the acceleration due to gravity, θ_0 is the ambient potential temperature, $\Delta\theta = \theta - \theta_0$ is the deficit of potential temperature in the drainage flow, u^+ is downslope (u^- is upslope) wind speed over a constant slope with angle α , $\overline{u'w'}(z)$ is momentum flux, $c_D(z)$ is drag coefficient, and h is a canopy height (for details see: Yi et al., 2005; Mahrt, 1982; Mahrt et al., 2000; 2001; Massman and Weil, 1999). These analytical models provide very simple but fundamental approaches to define links between canopy flow properties, topography and forest structure.

2.2. A super stable layer theory can be used to explain the conditions of canopy flow separation at night (Yi et al., 2005)

Our results have shown that there is a super stable layer of air during drainage flows immediately beneath the canopy layer with highest leaf area density. Our model predicts that this is due to a localized region of high wake-to-shear ratio, caused by the flow of air around the dense foliage. The super stable layer of air acts like a 'lid', preventing vertical exchange of the drainage flow beneath the canopy due to strong stratification. This also explains why the vertical advective CO₂ fluxes we previously observed at the site do not originate until near the top of the canopy, after the layer of maximum foliar density. The super stable layer of air also has the effect of constraining the drainage flows to a thin 'slab' that remains near the surface as it flows downslope. This was confirmed with the SF₆ tracer studies, which revealed little vertical mixing during downslope drainage flows. In summary, the super stable layer, a culprit in advection problems, is characterized by an local Richardson number approaching infinity, slow canopy flow, maximum drag force, horizontal CO₂ gradient and wake-to-shear ratio, and minimum vertical exchange. The super stable layer theory provides a physical basis to explain why horizontal advection is mainly restricted within canopy and vertical advection above canopy.

2.3. A numerical approach can be used to simulate terrain-induced flows within and above canopy (Yi et al., 2005)

We have successfully applied the renormalization-group k-epsilon turbulence model (Yakhot et al., 1992) to a forest environment with complex terrain in combination with our analytical derivations (Yi et al., 2005). The tentative results of computational fluid dynamics (CFD) experiments show three different dynamic regimes of topographic drainage flow that were simulated under different thermal-dynamic conditions (Figure 1). Cold inflow induces drainage flow in the lower part of canopy and strong stratification of airflows within entire canopy; additionally, the model predicts that there is a super stable layer around the maximum LAD level, which is consistent with our canopy flow theory (Figure 1a). This super stable layer minimizes vertical land-atmosphere exchange around the middle level of canopy. Warm inflow causes the rapid flushing of land-atmosphere exchange at the location where air motions converge, causing the 'chimney phenomenon' (Figure 1b). The oscillation of canopy flow occurs as the inflow temperature is close to the environmental temperature (Figure 1c).

2.4. A canopy buffer layer concept can be useful in understanding complex interactions between canopy flow and canopy structure

If terrain is flat, equation (2) becomes

$$-\overline{u'w'}(z)/u_*^2(h) = e^{-(LAI-L(z))} \quad (3)$$

where $u_*^2(h) = -\overline{u'w'}(h)$ is friction velocity at the top of canopy. Referring to Equation (3), the normalized Reynolds stress profile is completely determined by the **canopy buffer function**, $e^{-(LAI-L(z))}$ or, stated another way, canopy morphology.

The predictive ability of Equation (3) can be tested using previously published data on leaf area density and normalized Reynolds stress (Table 1). The calculated Reynolds stress profiles by Equation (3) using measured leaf area density profiles as input, accurately describe empirically-determined patterns (Figure 2). The overall comparison between predicted and measured Reynolds stress across eight canopies is shown in Figure 3 (predicted=0.9234*observed +0.0375; r=0.95, P<0.0001).

The comparison between the present model prediction and the higher-order closure model predictions is also illustrated in Figure 2a. The two higher order closure models include Wilson and Shaw's model (Wilson and Shaw, 1977) and Albin's model (Albin, 1981). The observed leaf area density data reported by Shaw (Shaw, 1977) were used in the three models for this comparison. Our simple model predicts the Reynolds stress profile equally as well, or better, than the more complicated higher order closure models.

The mechanistic basis to Equation (3) is found in the governing nature of canopy structure. The relative Reynolds stress at height z within the canopy is determined by the total leaf area in the screening layer as shown in Figure 4, i. e. by $LAI - L(z)$. A canopy buffer layer (CBL) is defined as a layer from the top of canopy to a level, z_B , at which 85% of the momentum at the top of canopy is extracted due to aerodynamic drag of the plant elements ($-\overline{u'w'}(z_B)/u_*^2(h) = 0.15$, Figure 4). The lower boundary z_B of the CBL can be solved from

$$\int_0^{z_B} \ell(z') dz' = LAI - 1.897, \quad (LAI \geq 1.897) \quad (7)$$

The relative CBL depth, $(h - z_B)/h$, is largely related to canopy morphology as shown in Figure 2. The up-side-down, funnel-shaped canopy like that designated "AS" in Figure 2c has a deep CBL, while the funnel-shaped canopy like that designated "HW" in Figure 2d has a shallow CBL. All the relative CBL depths estimated from Equation (7) are listed in Table 1. CBL is not only a layer that depletes the stress, but it also in breaks up larger-scale turbulent motions and converts them to smaller-scale wake motions. We have previously shown that the ratio of wake to shear production rate increases with decreasing of height within the CBL (Yi et al., 2005). The Reynolds stress below CBL is nearly constant as shown in Figure 2. The residual $\overline{R_{u'w'}/u_*^2}$ as defined in Figure 4, is equal to a value of the relative Reynolds stress at $z = 0$, and is determined by

$$\overline{R_{u'w'}/u_*^2} = e^{-LAI}. \quad (8)$$

The residual Reynolds stress decreases exponentially as LAI increases and approaches zero as $LAI \geq 5$ (Fig. 4).

Under the uniform vertical canopy condition, Equation (3) becomes:

$$\overline{u'w'}/u_*^2 = e^{-LAI(1-z/h)}. \quad (9)$$

The CBL depth is inversely proportional to LAI as

$$(h - z_B)/h = 1.897/LAI, \quad ((LAI \geq 1.897)). \quad (10)$$

The influence of LAI on the CBL depth is high in situations with relatively low LAI . The CBL depth is reduced by more than $1/2 h$ as LAI increases from 2 to 4 (Fig. 5).

3. Concluding remarks

We have developed analytical approaches to understand the complex interactions between canopy turbulent flows and canopy structure, and applied the CFD approach to simulate airflows around the forest environment. The model predictions for the Reynolds stress profiles were realistic and satisfactory in tests with data from eight morphologically distinct

canopies. The characteristics of canopy Reynolds stress profiles are reasonably determined by the LAI profile alone. The model is useful for predicting CBL depth, which is reflected in the fundamental reliance on canopy morphology and LAI . These analytical approaches provide some of avenues to assimilate direct observations within canopy layer into air quality and climate models. The fundamental physics behind these simple approaches have not been elucidated yet. The experimental and theoretical studies of these analytical approaches are all further invited.

4. Data

Data from observations of leaf area density and Reynolds stress, and predictions from higher-order closure models were taken from the literature (Wilson and Shaw, 1977; Albini, 1981; Katul and Albertson, 1998; Katul et al., 2004; Shaw et al., 1974, Wilson, 1988; Wilson et al., 1982; Amiro, 1990; Badocchi and Meyers, 1988; Baldocchi, 1989; Kelliher et al., 1998; 1999), by digitising published graphs when necessary. The experiments COa and COb were conducted in two different corn canopies in Elora, Ontario, Canada, respectively in 1971 (Wilson, 1988), and in 1976 and 1977 (Wilson et al., 1982; Amiro, 1990). The Reynolds stress profiles of COa were measured by using hot-film anemometers and COb by using specially-designed servo-controlled split-film heat-transfer anemometers. The observed stress data for COb were mean values for each measurement level from the Table 1 in Wilson et al. (1982). The experiments for AS (aspens), JPI (Jack pine) and SP (spruce) were conducted in three different boreal forest canopy sites near Whiteshell Nuclear Research Establishment in south-eastern Manitoba, Canada (Amiro, 1990). The Reynolds stress profiles were measured by two triaxial sonic anemometers (Applied Technology Inc, Boulder, CO, USA), one was operated above the forest while the other was roving at different heights. The experiments for HW (oak-hickory-pine) were conducted near Oak Ridge, Tennessee, USA (Badocchi and Meyers, 1988; Baldocchi, 1989). The Reynolds stress profiles were measured using three simultaneous Gill sonic anemometers. The experiments for LPI (loblolly pine) were conducted at the Blackwood division of the Duke Forest near Durham, North Carolina, USA (Katul and Albertson, 1998). The Reynolds stress profiles were simultaneously measured at six levels using five Campbell Scientific CSAT3 (Campbell Scientific, Logan Utah, USA) triaxial sonic anemometers within canopy and a Solent Gill sonic anemometer above canopy. The experiments for SPI (Scott pine) were carried out at 40 km southwest of the village of Zotino along the western bank of the Yenisei River in central Siberia, Russia (Kelliher et al., 1998; 1999). The Reynolds stress profiles were measured using five sonic anemometers (Solent R3, Gill Instruments, Lymington, UK). All leaf area density profiles were measured across the eight sites either by destructive harvest or using plant canopy analyzers (LiCor 2000, Lincoln, Nebraska, USA).

5. References

- Albini, F. A. A. (1981), phenomenological model for wind speed and shear stress profiles in vegetation cover layers, *Journal of Applied Meteorology*, 20, 1325–1335.
- Amiro, B. D. (1990) Comparison of Turbulence Statistics within 3 Boreal Forest Canopies, *Boundary-Layer Meteorology* 51, 99–121.

- Baldocchi, D.D et al. (2001), Fluxnet: a new tool to study the temporal and spatial variability of ecosystem-scale carbon dioxide, water vapor, and energy flux densities. *Bulletin of the American Meteorological Society*, 82, 2415-2434.
- Baldocchi, D. D. & Meyers, T. D. (1988) A Spectral and Lag-Correlation Analysis of Turbulence in a Deciduous Forest Canopy. *Boundary-Layer Meteorology* 45, 31–58.
- Baldocchi, D. D. (1989) Turbulent Transfer in a Deciduous Forest. *Tree Phys.* 5, 357–377.
- Finnigan J.J. (2004) A re-evaluation of long-term flux measurement techniques Part 2: Coordinate systems, *Boundary-Layer Meteorology*, 113, 1-41.
- Finnigan, J.J. (2006) Modeling stably stratified flows over vegetated topography, iLEAPS Specialist Workshop on “Flux Measurements in Difficult Conditions”, 26-28 January 2006, NCAR Center Green Campus, Boulder, Colorado, USA.
- Goulden, ML, Munger JW, Fan SM, Daube BC, and Wofsy SC (1996) Measurements of carbon sequestration by long-term eddy covariance: methods and a critical evaluation of accuracy. *Global Change Biology*, 2, 169-182.
- Goulden, ML, Miller S.D., and da Rocha H.R. (2006) The underestimation of CO₂ flux on calm nights: Amazonian rainforest as extreme case study, iLEAPS Specialist Workshop on “Flux Measurements in Difficult Conditions”, 26-28 January 2006, NCAR Center Green Campus, Boulder, Colorado, USA.
- Kelliher, F. M. et al. (1998) Evaporation from a Central Siberian Pine Forest. *J. Hydrol.* 205, 279–296.
- Kelliher, F. M. et al. (1999) Carbon Dioxide Efflux Density from the Floor of a Central Siberian Pine Forest. *Agricultural and Forest Meteorology* 94, 217–232.
- Mahrt, L (1982) Momentum balance of gravity flows, *J. Atmos. Sci.*, 39, 2701–2711.
- Mahrt, L, Lee X., Black A., Neumann H., and Staebler R.M. (2000) Nocturnal mixing in a forest subcanopy, *Agricultural and Forest Meteorology*, 101, 67-78.
- Mahrt, L, Vickers D., Sun J., Jensen N.O., Jorgensen H., Pardyjak E., and Fernando H. (2001) Determination of the surface drag coefficient, *Boundary-Layer Meteorol.*, 99, 249-276.
- Mahrt, L. (2006) Spatial and temporal intermittency of exchange processes including mesoscale transport, iLEAPS Specialist Workshop on “Flux Measurements in Difficult Conditions”, 26-28 January 2006, NCAR Center Green Campus, Boulder, Colorado, USA.
- Massman, W.J., and Weil J.C. (1999) An analytical one-dimensional second-order closure model of turbulence statistics and the Lagrangian time scale within and above plant canopies of arbitrary structure, *Boundary-Layer Meteorology*, 91, 81-107.
- Massman WJ, and Lee X. (2002) Eddy covariance flux corrections and uncertainties in long-term studies of carbon and energy exchanges. *Agricultural and Forest Meteorology*, 113, 121-144.
- Shaw, R.H (1977) Secondary wind speed maxima inside plant canopies, *J. Appl. Meteor.*, 16, 514-521.
- Shaw, R.H, Silversides, R. H. & Thurtell, G. W. (1974) Measurements of mean wind flow and three-dimensional turbulence intensity within a mature corn canopy. *Agricultural Meteorology* 13, 417-425.
- Wilson, N.R. and R.H. Shaw (1977) A higher order closure model for canopy flow, *Journal of Applied Meteorology*, 16, 1197-1205.
- Wilson, J. D. (1988) A 2nd-Order Closure Model for Flow through Vegetation. *Boundary-Layer Meteorology* 42, 371–392.
- Wilson, J. D., Ward, D. P., Thurtell, G. W. & Kidd, G. E. (1982) Statistics of Atmospheric Turbulence within and above a Corn Canopy. *Boundary-Layer Meteorology* 24, 495–519.
- Yakhot, V., Orzag S.A., Thangam S., Gatski T.B., and Speziak C.G. (1992) Development of Turbulence Models for Shear Flows by a Double Expansion Technique, *Physics Fluids A*, 4, 1510-1520.
- Yi, C., R. K. Monson, Z. Zhai, D. E. Anderson, B. Lamb, G. Allwine, A. A. Turnipseed, and S. P. Burns (2005) Modeling and measuring the nocturnal drainage flow in a high-elevation, subalpine forest with complex terrain, *Journal of Geographical Research*, 110, D22303, doi:10.1029/2005JD006282, 2005.
- Yi, C., Monson K.R., Anderson D.E., Turnipseed A.A., and Burns S.P., The contribution of advective fluxes to net ecosystem CO₂ exchange in a high-elevation, subalpine forest ecosystem, in preparation for *Ecological Applications*, 2006.

Table 1. Canopy morphology and characteristics of the Reynolds stress profile.

Canopy	COa ¹⁴	COb ¹⁵⁻¹⁶	AS ¹⁶	HW ¹⁷⁻¹⁸	JPI ¹⁶	LPI ⁸	SP ¹⁶	SPI ¹⁹⁻²⁰
h (m)	2.9	2.2	10	22	15	16	10	20
LAI (m² m⁻²)	3.0	2.9	4.0	5.0	2.0	3.8	10.0	2.6
$\Delta h_{CBL}/h$	0.57	0.50	0.54	0.14	0.55	0.44	0.23	0.40
$R_{\overline{u'w'}/u_c^2}$	0.050	0.055	0.018	0.007	0.135	0.022	0.000	0.074

COa and COb are different corn canopies, AS is the aspen stand, HW is the hardwood forest, JPI is the Jack pine stand, LPI is the Loblolly pine stand, SP is the spruce stand, and SPI is the Scots pine stand. Details of sites and measurements are described in the indicated references. $\Delta h_{CBL}/h$ is the relative CBL depth. $R_{\overline{u'w'}/u_c^2}$ is a residual term as defined in Equation (8)

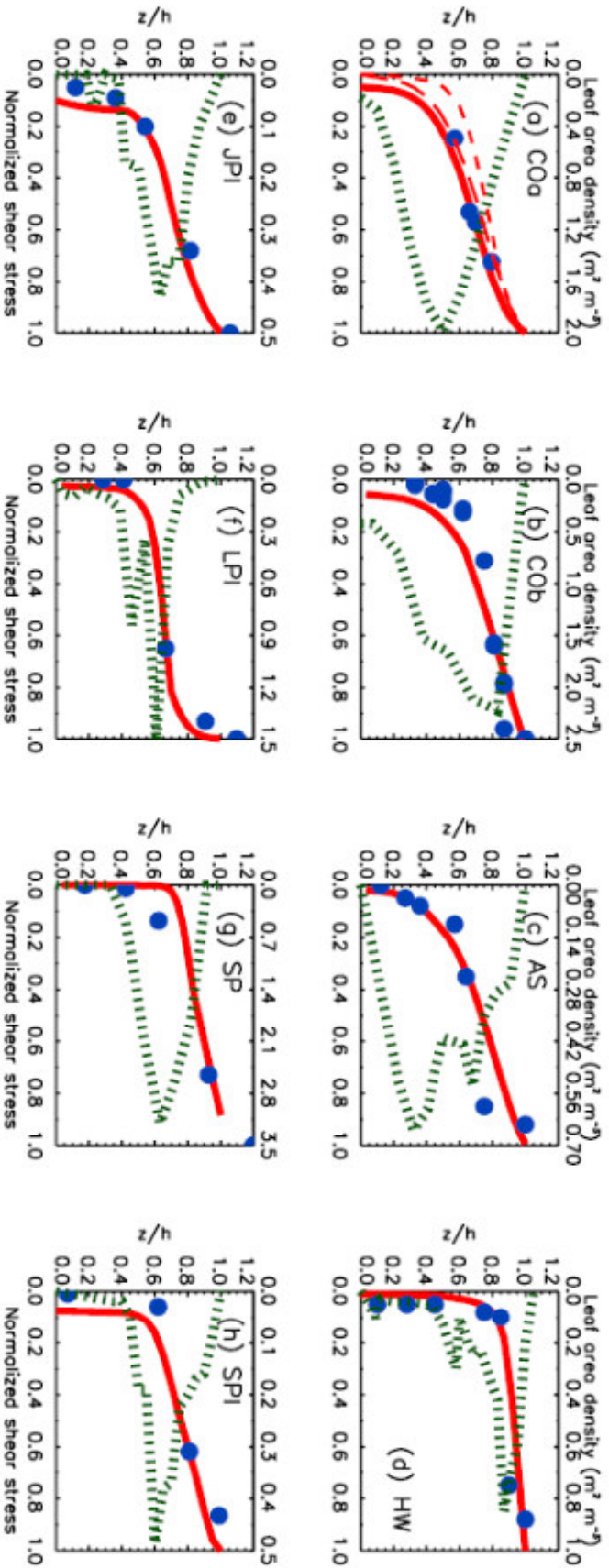


Figure 2. Comparison of predicted normalized Reynolds stress profiles from the present model (solid line) to observed data (filled circle) (WHAT IS THE FAT DOTTED LINE?-THERE ARE 4 LINES IN SOME FIGS) in eight vegetation types (see Table 1) reported in literature^{8-9, 13-20}. The comparison of the prediction between present model and the higher order closure models is also shown in (a), the long dashed line was predicted by Wilson and Shaw's model⁵ and dashed line by Albini's model⁷.

